Research article

Journal of Physical Organic Chemistry

Received: 8 February 2015, Revised: 6 May 2015, Accepted: 26 June 2015, Published online in Wiley Online Library: 4 August 2015

(wileyonlinelibrary.com) DOI: 10.1002/poc.3477

Palladium-catalyzed cyclization of 2-alkynyl-*N*-ethanoyl anilines to indoles: synthesis, structural, spectroscopic, and mechanistic study

Mohammad Mazharol Hoque[a,b], Mohammad A. Halim[b]*, Mohammed G. Sarwar[c] and Md. Wahab Khan[a]**

This study reports a facial regio-selective synthesis of 2-alkyl-*N*-ethanoyl indoles from substituted-*N*-ethanoyl anilines employing palladium (II) chloride, which acts as a cyclization catalyst. The mechanistic trait of palladium-based cyclization is also explored by employing density functional theory. In a two-step mechanism, the palladium, which attaches to the ethylene carbons, promotes the proton transfer and cyclization. The gas-phase barrier height of the first transition state is 37 kcal/mol, indicating the rate-determining step of this reaction. Incorporating acetonitrile through the solvation model on density solvation model reduces the barrier height to 31 kcal/mol. In the presence of solvent, the electron-releasing ($-CH_3$) group has a greater influence on the reduction of the barrier height compared with the electron-withdrawing group (–Cl). These results further confirm that solvent plays an important role on palladium-catalyzed proton transfer and cyclization. For unveiling structural, spectroscopic, and photophysical properties, experimental and computational studies are also performed. Thermodynamic analysis discloses that these reactions are exothermic. The highest occupied molecular orbital–lowest unoccupied molecular orbital gap (4.9–5.0 eV) confirms that these compounds are more chemically reactive than indole. The calculated UV–Vis spectra by time-dependent density functional theory exhibit strong peaks at 290, 246, and 232 nm, in good agreement with the experimental results. Moreover, experimental and computed ^1H and ^{13}C NMR chemical shifts of the indole derivatives are well correlated. Copyright © 2015 John Wiley & Sons, Ltd.

Keywords: cross-coupling; density functional theory (DFT); indole derivatives; palladium catalysis; time-dependent density functional theory (TD-DFT); transition states

INTRODUCTION

The substituted indoles, both naturally occurring and synthetic, exhibit a wide range of biological activity.[1–5] They have been referred to as a "privileged structure" because of their excellent binding ability with various receptors.[6,7] This is a reason why indole derivatives have become structural motifs in many pharmaceuticals and agrochemical products.[8] Serotonin, a simple indole derivative, acts as a neurotransmitter,[9] and vinblastine, a complex alkaloid therapeutic agent, is used clinically as an anticancer agent.[10–12] Moreover, a number of important synthetic drugs contain an indole motif. For example, fluvastatin is used to treat hypercholesterolemia as well as to prevent cardiovascular disease[13]; 5-chloro-3-{(3, 5-dimethylphenyl)sulfunyl}-4-fluoro-1*H*-indole-2-carboximate[14] and methyl (2-carbamoyl-5-chloro-1H-indol-3yl) (phenyl) phosphinate are potent inhibitors of HIV-1.[15] Furthermore, Indole-3-Carbinol, a simple molecule present in wide range of plants, has modest activity against the glioma cell lines 132N1 and U87MG.[16]

Besides medicinal or therapeutic activities, many proteins contain indole skeletons; for example, tryptophan – an essential aromatic amino acid in the human diet – is a component of many structural or enzyme proteins. It has been reported that indole and tryptophan with hydroxyl groups on the six-member aromatic ring were found to have lower oxidation potentials than their parent compounds. Hence, it produces the least amount of H_2O_2 upon light exposure and is capable of protecting tryptophan from oxidation in mAb1 against diverse reactive oxygen species, which may lead to formulation of applications in protection of proteins against degradation via oxidation.[17] Nowadays, dye-sensitizing solar cells (DSSCs) have attracted common interest as a new renewable energy source because of their low cost and high efficiency.[18–22] A recent investigation on

* *Correspondence to: Mohammad A. Halim, Bangladesh Institute of Computational Chemistry and Biochemistry, 38 Green Road West, Dhaka 1205, Bangladesh.*
E-mail: bdcomputchem@gmail.com

** *Correspondence to: Md. Wahab Khan, Department of Chemistry, Bangladesh University of Engineering and Technology, Dhaka 1000, Bangladesh.*
E-mail: mwkhan@chem.buet.ac.bd

a *M. M. Hoque, M. W. Khan*
Department of Chemistry, Bangladesh University of Engineering and Technology, Dhaka 1000, Bangladesh

b *M. M. Hoque, M. A. Halim*
Bangladesh Institute of Computational Chemistry and Biochemistry, 38 Green Road West, Dhaka 1205, Bangladesh

c *M. G. Sarwar*
Department of Chemistry, The Scripps Research Institute, La Jolla, CA, 92037, USA

the photovoltaic performance of LI-3 and LI-4 in DSSCs demonstrated the overall efficiency of 4.31%, compared with the standard cell from N719 (7.88%) under the same condition.[23]

Because of the great importance and diverse applications, the continued development of routes toward indoles has been a central theme in organic synthesis over the last century.[24–27] Palladium-catalyzed protocols have played significant role for the synthesis of functionalized indole from simple and commercially accessible starting materials.[28–34] The most commonly used palladium (II) salts in indole chemistry are $PdCl_2$ and $Pd(OAc)_2$, generally employed as $PdCl_2(PPh_3)_2$, $Pd(OAc)_2(PPh_3)_2$, and $PdCl_2(MeCN)_2$. In numerous transformations, aryl iodide has widely been used as a synthetic intermediate. A microwave-assisted two-step reaction was carried out under Sonogashira coupling conditions from *N*-substituted/*N*,*N*-disubstituted iodo anilines and terminal alkynes followed by the addition of acetonitrile and aryl iodide to synthesize polysubstituted indoles.[35] In addition, the direct synthesis of indole from anilines and ketones has been carried out, employing $Pd(OAc)_2$ with $Cu(OAc)_2$ as a stoichiometric co-oxidant.[36] In recent years, our group has developed methods for the synthesis of benzo-fused heterocyclic compounds including isoindolines, isoquinolinone,[37] benz[b]furans,[38] and indoles,[39] by palladium-catalyzed reactions of aryl iodide with terminal alkynes.[40]

As the substituted indole nucleus is a structural component of a vast number of biologically active and functional materials and natural and synthetic compounds, we are therefore interested in developing a convenient method for the synthesis. For exploring detail structural, spectroscopic, and photophysical properties, density functional theory (DFT) and time-dependent DFT (TD-DFT) are employed. The mechanistic feature of palladium (II) chloride-based cyclization to form 2-alkyl-*N*-ethanoyl indole is also investigated by locating transition states.

EXPERIMENTAL AND COMPUTATIONAL METHODS

General experimental

Melting points were determined in open capillary tubes on Gallenkamp (London, England) melting point apparatus and are uncorrected. Infrared (IR) spectra were recorded on a Shimadzu (Kyoto, Japan) Fourier transform infrared (FTIR) spectrophotometer (range: 4000–400/cm and number of scans: 45), and UV spectra were recorded in dry EtOH with a Shimadzu (Kyoto, Japan) visible spectrophotometer. ^{1}H NMR and ^{13}C NMR spectra were recorded on a Bruker (Billerica, MA, USA) DPX-400 spectrophotometer (400 MHz) using tetramethylsilane as an internal reference. Analytical thin layer chromatography (TLC) was performed on pre-coated silica gel 60 F_{254} (E. Merck, Darmstadt, Germany), and the spots were visualized with UV light. Column chromatography was performed on silica gel (60–120 mesh). Reagents were purchased from E. Merck and Fluka (St Gallen, Switzerland).

Synthesis of starting materials substituted-2-iodoacetanilides 1 and 2

In our recent study, we developed a method of one-pot synthesizing 2-iodoacetanilide, which has been employed to prepare the required starting materials **1** and **2** of our present study using iodine–copper (II) acetate in acetic acid from their parent substituted anilines.

2-Iodo-4-methylacetanilide ***1***

Brown crystal; Mp. 125–128 °C; IR (KBr): ν_{max} 3265.3, 1654.8, 1523.7, 1290.3 cm^{-1}; UV (EtOH): λ_{max} 401.85, 199.99 nm; ^{1}H NMR (400 MHz, $CDCl_3$): δ_H 7.99 (d, 1H, J = 8.0 Hz), 7.59 (s, 1H), 7.32 (br s, 1H), 7.12 (d, 1H, J = 8.0 Hz), 2.26 (s, 3H), 2.10 (s, 3H); ^{13}C NMR (100 MHz, $CDCl_3$): δ_c 168.15, 145.98, 138.96, 135.79, 129.92, 122.12, 90.29, 24.67, 20.30.

4-Chloro-2-iodoacetanilide ***2***

White crystal; IR (KBr): ν_{max} 3274.9, 1658.7, 1577.7, 1568.0, 1521.7, 1463.9 1375.2, 1288.4 cm^{-1}; ^{1}H NMR (400 MHz, $CDCl_3$): δ_H 8.15 (d, 1H, J = 8.0 Hz), 7.74 (d, 1H, J = 2.0 Hz), 7.36 (br s, 1H), 7.30 (dd, 1H, J = 8.0 and 2.0 Hz, H-5), 2.22 (s, 3H); UV (EtOH): λ_{max} 240.65, 200.15 nm.

General procedure for the synthesis of substituted-2-(1-alkynyl)acetanilides, 5–7

In a 50-mL round bottom flask equipped with a reflux condenser, a mixture of 2-iodo-4-methyl-*N*-ethanoyl aniline **1** (0.5 g, 1.818 mmol), bis(triphenylphosphine) palladium (II) chloride (0.044 g, 0.063 mmol), copper (I) iodide (0.027 g, 0.145 mmol), and triethylamine (0.734 g, 7.272 mmol) was stirred in 7-ml dimethylformamide (DMF) under a nitrogen atmosphere for 1 h at room temperature. Then, 1-heptyne **3** (0.178 g, 2.181 mmol) was added, and the solution was heated at 60 °C for 48 h. The mixture was then evaporated to dryness under reduced pressure. The residue was extracted with chloroform (3 × 50 mL), and the combined chloroform extracts were washed with distilled water (3 × 50 mL), dried over anhydrous Na_2SO_4, filtered, and concentrated under reduced pressure. The residue was purified by column chromatography on silica gel using n-hexane/ethyl acetate (8:1) to yield the pure 2-(1-heptynyl)-4-methyl-*N*-ethanoyl aniline **5** (Scheme 1).

2-(1-Heptynyl)-4-methyl-N-ethanoyl aniline, ***5***

Brown crystalline solid; Mp. 64–65 °C; IR (KBr): ν_{max} 3274.9, 2933.5, 2219.9, 1662.5, 1522.5 cm^{-1}; UV (EtOH): λ_{max} 365.5, 284 nm; ^{1}H NMR (400 MHz, $CDCl_3$): δ_H 8.21 (d, 1H, J = 8.4 Hz), 7.84 (br s, 1H), 7.16 (s, 1H), 7.07 (d, 1H, J = 8.0 Hz), 2.48 (t, 2H, J = 6.8 Hz), 2.25 (s, 3H), 2.18 (s, 3H), 1.64 (quint, 2H, J = 7.2 and 6.8 Hz), 1.49–1.24 (m, 4H), 0.92 (t, J = 7.2 Hz); ^{13}C NMR (100 MHz, $CDCl_3$): δ_c 167.94, 136.48, 132.73, 131.80, 129.59, 118.91 and 112.38, 97.42, 76.09, 31.18, 28.47, 24.90, 22.24, 20.64, 19.55, 14.01.

2-(1-Hexynyl)-4-methyl-N-ethanoyl aniline, ***6***

Brown crystalline solid; Mp. 84–86 °C; IR (KBr): ν_{max} 3274.9, 2956.7, 2933.5, 2223.8, 1664.5, 1587.3, 1525.6, 1488.9, 1363.6, 1301.9, 829.3 cm^{-1}; UV (EtOH): λ_{max} 308, 265.2, 263.6, 260.4 nm; ^{1}H NMR

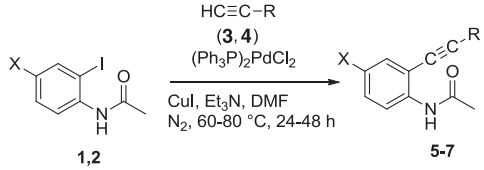

1, 5, 6, X = CH_3; **2, 7,** X = Cl **4,7,** R = n-C_4H_9 **3, 5,** R = n-C_5H_{11}

Scheme 1. Synthesis of substituted-2-(1-alkynyl)acetanilides

(400 MHz, $CDCl_3$): δ_H 8.21 (d, 1H, J = 8.4 Hz), 7.84 (br s, 1H), 7.15 (s, 1H), 7.07 (d, 1H, J = 8.4 Hz), 2.49 (t, 2H, J = 7.2 Hz), 2.25 (s, 3H), 2.17 (s, 3H), 1.63 (quint, 2H, J = 7.2 and 6.8 Hz), 1.50 (sex, 2H, J = 7.2 and 6.8 Hz), 0.96 (t, 3H, J = 7.2 Hz); ^{13}C NMR (100 MHz, $CDCl_3$): δ_c 167.91, 136.54, 132.74, 131.81, 129.59, 118.99, 112.46, 97.33, 76.17, 30.83, 24.83, 22.08, 20.63, 19.25, 13.59.

4-Chloro-2-(1-hexynyl)-N-ethanoyl aniline, ***7***

White crystalline solid; Mp. 80–82 °C; IR (KBr): 3294.2, 2956.7, 2927.7, 2223.8, 1662.5, 1598.9, 1473.5 cm^{-1}; UV (EtOH): λ_{max} 300.5, 284 nm; ^{1}H NMR (400 MHz, $CDCl_3$): δ_H 8.31 (d, 1H J = 8.8 Hz), 7.85 (br s, 1H, 7.31 (d, 1H, J = 2.0 Hz), 7.21 (dd, 1H, J = 8.8 and 2.0 Hz), 2.49 (t, 2H, J = 6.8 Hz), 2.18 (s, 3H), 1.62 (quint, 2H, J = 6.8 and 7.2 Hz), 1.50 (sex, 2H, J = 7.2 and 7.6 Hz), 0.96 (t, 3H, J = 7.6 Hz); ^{13}C NMR (100 MHz, $CDCl_3$): δ_c 168.01), 137.50, 131.05, 128.87, 127.98, 120.12, 114.09, 99.07, 74.94, 30.63, 24.82, 22.06, 19.22, 13.55.

General methods for $PdCl_2$-catalyzed synthesis of 2,5-disubstituted-*N*-ethanoyl indoles 8–10

In a 50-mL round bottom flask equipped with a reflux condenser, a mixture of palladium (II) chloride (0.006 g, 0.032 mmol) and acetonitrile (5 mL) was refluxed at 80 °C with constant stirring. The solid dissolved after 20 min, and the reaction mixture was allowed to cool at room temperature. In this solution (0.076 g, 0.315 mmol) of 2-(1-heptynyl)-4-methyl-*N*-ethanoyl aniline **5** was added and the mixture was refluxed at 80 °C. The progress of the reaction was monitored by TLC. The starting material disappeared after 40 min, and the reaction mixture was evaporated to dryness under reduced pressure. The product was purified by column chromatography on silica gel using n-hexane/ethyl acetate (5:1) to yield 0.056 g of the pure 5-methyl-2-pentyl-*N*-ethanoylindole **8**.

2-Pentyl-5-methyl-N-ethanoyl indole, ***8***

White crystalline solid; Mp. 50–51 °C; IR (KBr): ν_{max} 2921.9, 1687.6, 1591.2, 1460.70, 1373.2, 1315.4, 815.8 cm^{-1}; UV (EtOH): λ_{max} 371.4, 304.0, 293.5 nm; ^{1}H NMR (400 MHz, $CDCl_3$): δ_H 7.68 (d, 1H, J = 8.4 Hz), 7.25 (s, 1H), 7.04 (d, 1H, J = 8.4 Hz), 6.32 (s, 1H), 2.97 (t, 2H, J = 7.6 Hz), 2.72 (s, 3H), 2.41 (s, 3H), 1.69 (quint, 2H, J = 7.2 and 7.6 Hz'), 1.42–1.28 (m, 4H), 0.96 (t, J = 7.2 Hz); ^{13}C NMR (100 MHz, $CDCl_3$): δ_c 170.19, 143.21, 134.61, 132.49, 130.31, 124.59, 120.20, 114.48, 108.03, 31.67, 30.55, 28.62, 27.57, 22.56, 21.12, 14.05; anal. calcd. for $C_{16}H_{21}NO$: C, 78.97; H, 8.70. Found: 78.91; H, 8.71.

2-Butyl-5-methyl-N-ethanoyl indole, ***9***

White crystalline solid; Mp. 68–69 °C; IR (KBr): ν_{max} 2958.6, 2935.5, 1679.9, 1591.2, 1469.7 1379.4, 1317.3 cm^{-1}; UV (EtOH): λ_{max} 366.5, 304.0, 295.5 nm; ^{1}H NMR (400 MHz, $CDCl_3$): δ_H 7.68 (d, 1H, J = 8.4 Hz), 7.25 (s, 1H), 7.04 (d, 1H, J = 8.4 Hz), 6.32 (s, 1H), 2.98 (t, 2H, J = 7.6 Hz), 2.72 (s, 3H), 2.41 (s, 3H), 1.68 (quint, 2H, J = 7.2 and 7.6 Hz), 1.44 (sex, 2H), 0.95 (t, 3H, J = 7.2 Hz); ^{13}C NMR (100 MHz, $CDCl_3$): δ_c 170.19, 143.18, 134.60, 132.49, 130.31, 124.59, 120.20, 114.48, 108.03, 31.07, 30.30, 27.57, 22.56, 21.11, 13.97; anal. calcd. for $C_{15}H_{19}NO$: C, 78.56; H, 8.35. Found: 78.48; H, 8.39.

2-Butyl-5-chloro-N-ethanoyl indole, ***10***

White crystalline solid; Mp. 51–52 °C; IR (KBr): ν_{max} 2937.4, 1685.7, 1591.2, 1448.4, 1371.3, 1317.3, 829.3 cm^{-1}; UV (EtOH): λ_{max} 352.5, 305.0, 291.0 nm; ^{1}H NMR (400 MHz, $CDCl_3$): δ_H 7.80 (d, 1H, J = 9.2 Hz), 7.42 (d, 1H, J = 2.0Hz), 7.17(dd, 1H, J = 9.2 and 2.0 Hz), 6.34 (s, 1H), 2.96 (t, 2H, J = 7.2 Hz), 2.72 (s, 3H), 1.69 (quint, 2H, J = 7.2 and 7.6 Hz), 1.44 (sex, 2H, J = 7.2 and 7.6 Hz), 0.96 (t, 3H, J = 7.6 Hz); ^{13}C NMR (100 MHz, $CDCl_3$): δ_c 170.05, 144.13, 134.90, 131.20, 128.63, 123.47, 119.63, 115.94, 107.52, 30.96, 30.22, 27.48, 22.55, 13.93; anal. calcd. for C14H_{16}ClNO: C, 67.33; H, 6.46. Found: 67.10; H, 6.45.

General procedure for the synthesis of substituted-1H indoles, 9a and 10a, by base-catalyzed reaction.

A mixture of substituted 2-alkynylacetanilides, **21–24** (1 mmol), and sodium ethoxide (1.2–1.5 mmol) in 20-mL ethanol was stirred under a nitrogen atmosphere for 4 h at 80 °C. The reaction mixture was evaporated to dryness under reduced pressure. After usual workup, the residue was purified by column chromatography on silica gel using n-hexane/ethylacetate as eluant to yield substituted-1*H*-indoles **9a** and **10a** (Scheme 2).

2-Butyl-5-methyl-1H-indole, ***9a***

Pale yellow liquid; IR (KBr): ν_{max} 3408.0, 2956.7, 2929.7, 1618.2, 1502.4, 1458.1 cm^{-1}; ^{1}H NMR (400 MHz, $CDCl_3$): δ 7.75 (br s, 1H), 7.29 (s, 1H), 7.16 (d, 1H, J = 8.0 Hz), 6.91 (d, 1H, J = 8.0 Hz), 6.45 (s, 1H), 2.72 (t, 2H, J = 7.6 Hz), 2.41 (s, 3H), 1.68 (quint, 2H, J = 7.6, 7.2 Hz, H-2'), 1.39 (sex, 2H, J = 7.2, 7.6 Hz), 0.87 (t, 3H, J = 7.2 Hz).

2-Butyl-5-chloro-1H-indole, ***10a***

Pale brown liquid, yield; IR (KBr): ν_{max} 3421.5, 2958.6, 2929.7, 1488.9 cm^{-1}; ^{1}H NMR (400 MHz, $CDCl_3$): δ 7.87 (s, 1H), 7.46 (s, 1H), 7.17 (d, 1H, J = 8.4 Hz), 7.04 (d, 1H, J = 8.4 Hz), 6.13 (s, 1H), 2.73 (t, 2H, J = 7.6 Hz), 1.69 (quint, 2H, J = 7.2 and 7.6 Hz), 1.39 (sex, 2H, J = 7.2, 7.6 Hz), 0.95 (t, 3H, J = 7.2 Hz).

Computational details

All calculations were carried out using the Gaussian 09 program package (Gaussian Inc., Wallingford, CT, USA).[41] The equilibrium geometry of compounds **5–10** were optimized at the B3LYP/6-31+G(d, p) level of theory, and subsequently vibrational frequencies were calculated. A scaling factor of 0.9648 was applied to the computed vibrational frequencies in order to compare with experimental results.[42,43] The optimized structures **8–10** were used to compute the lowest 10 singlet → singlet spin-allowed electronic vertical excitation energies by TD-DFT using B3LYP/6-31+G(d, p), CAM-B3LYP/6-31+G(d, p), M06/6-31+G(d, p), and X3LYP/6-31+G(d, p) level of theories. However, X3LYP/6-31+G(d, p) showed the best agreement

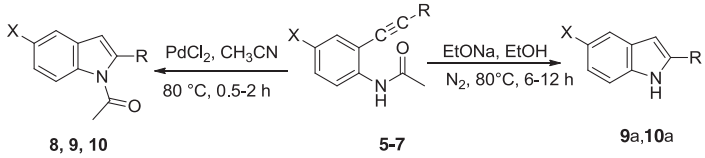

5, **6**, **8**, **9**, **9**a, X = CH_3 **7**, **10**, **10**a X = Cl **6**, **7**, **9**, **9**a, **10**, **10**a, R = n-C_4H_9 **5**, **8**, R = n- C_5H_{11}

Scheme 2. Synthesis of 2,5-disubstituted-*N*-ethanoyl indoles and substituted-1*H* indoles

with the experimental UV–Vis results. Chemical shift values of hydrogen and carbon were performed, employing the gauge-including atomic orbital approach and using 6-311+G(2d) basis set in $CHCl_3$. The transition states related to the palladium (II) chloride-catalyzed cyclization of 2-alkynal-4-substituted-*N*-ethanoyl acetanilides to 2-alkyl-5-substituted-*N*-ethanoyl indoles were optimized at the B3LYP/SDD level of theory. All transition states have a single imaginary frequency. An intrinsic reaction coordinate calculation has been performed to connect the transition states with their corresponding reactant, intermediates, and product. Single-point calculation with B3LYP/SDD level of theory was performed to test the solvent effect on this reaction mechanism employing conductor-like polarizable continuum model (CPCM)[44,45] and solvation model on density (SMD)[46] solvation models, where acetonitrile has been used as the solvent. SMD provides the best result on stabilizing the transition state, intermediate, and product.

RESULTS AND DISCUSSION

Synthesis and related discussion of 2-alkyl-5-substituted-*N*-ethanoyl indoles

Here, we report a new approach for the regio-selective synthesis of 2-alkyl-4-substituted-*N*-ethanoyl indoles **8–10** by palladium-catalyzed reaction (Table 1a). Recently, we described a facile and efficient one-pot iodination of aryl amines synthesizing substituted 2-iodoacetanilides.[47] In this study, 2-iodoacetanilides **1** and **2**, which contain an *N*-acetyl as a protecting group of the amine function, have been used as intermediates for coupling with 1-alkynes **3** and **4** in the presence of bis(triphenylphosphine) palladium (II) chloride (3.5 mol%), copper (I) iodide (8 mol%), and triethylamine (4 mol equiv.) under nitrogen atmosphere in DMF (5–8 mL) at 60–80 °C for 24–48 h. This reaction produces 2-alkynal-4-substituted-*N*-ethanoyl anilines **5–7** with good yield (60–72%).

To explore the generality of the coupling reaction, different 1-alkynes can be employed. It is observed that 1-hexyne **4** has relatively short reaction time (36 h) and high yield (72%), whereas 1-heptyne **3** takes a longer time (48 h) and produces a comparatively low yield (60%). The result indicates that the short-chain terminal alkynes are more reactive than the long-chain terminal alkynes. In addition, the substituent (X) groups in 2-iodoacetanilide (Scheme 1) also have significant impact. In the coupling reaction, acetanilide **1** with substituent *p*-CH_3 resulted in higher yields and greater kinetic reactivity than acetanilide **2** with substituent *p*-Cl in same reaction conditions.

The cyclization of 2-alkynyl-*N*-ethanoyl anilines were usually carried out by heating a mixture of palladium (II) chloride (10 mol%) in acetonitrile. In order to optimize the cyclization reaction, various catalysts along with solvents were employed (Scheme 2 and Table 1b).

Heating a mixture of 2-alkynyl-*N*-ethanoyl anilines **5–7** with palladium (II) chloride (10 mol%) in acetonitrile at 80 °C for 0.5–2 h produced 2,5-disubstituted-*N*-ethanoyl indoles **8**, **9**, and **10**. Other palladium catalysts such as bis(triphenylphosphine) palladium (II) with co-catalyst copper (I) iodide, in the presence of base triethylamine in DMF under nitrogen atmosphere at 80 °C, were not able to yield an indole compound for 2-alkynyl-*N*-ethanoyl aniline **6**. However, sodium ethoxide (1.2 mol equiv.) in ethanol under a nitrogen atmosphere at 80 °C for 4–12 h was found to be a potential catalytic system for annulations of 2-alkynyl-*N*-ethanoyl anilines **6** and **7** to give in **9a** and **10a**, but this protocol provides an inadequate yield percent.

Table 1a. Synthesis of substituted-2-alkynyl-*N*-ethanoyl anilines and substituted indoles

Substituted-2-iodoacetanilide	Alkyne-1	Substituted 2-alkynyl-*N*-ethanoyl aniline[a]	Substituted indole[b]	% yield a(b)
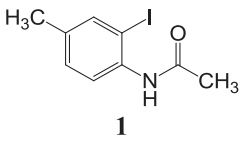 **1**	$HC{\equiv}C-(CH_2)_4CH_3$ **3**	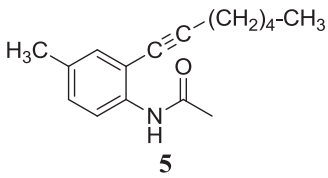 **5**	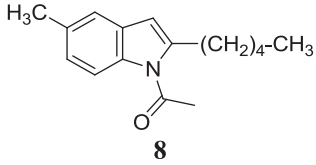 **8**	60(74)
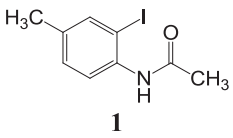 **1**	$HC{\equiv}C-(CH_2)_3CH_3$ **4**	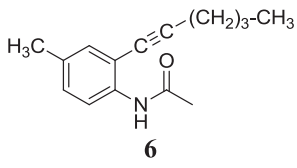 **6**	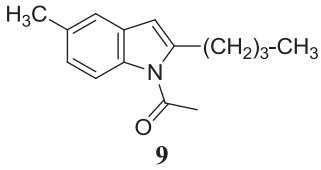 **9**	72(71)
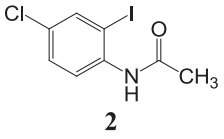 **2**	$HC{\equiv}C-(CH_2)_3CH_3$ **4**	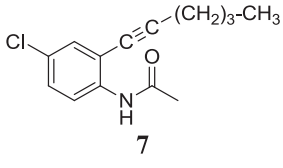 **7**	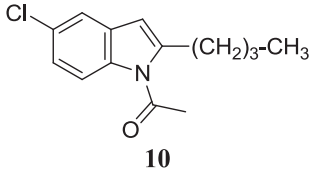 **10**	68(68)

[a]Isolated yield out of bracket based on substituted-2-iodoacetanilide.
[b]Isolated yield in bracket based on substituted 2-alkynyl-*N*-ethanoyl aniline.

Table 1b. Effect of catalyst on cyclization of 2-alkynyl-*N*-ethanoyl anilines to indoles

2-Alkynyl-*N*-ethanoyl anilines			Conditions	Indoles	
Compounds	R	X		Compounds	Yield (%)
5	n-C_5H_{11}	CH_3	$PdCl_2$ (10 mol%), CH_3CN, 80 °C, 0.75 h	**8**	68
6	n-C_4H_9	CH_3	$PdCl_2$ (10 mol%), CH_3CN, 80 °C, 0.5 h	**9**	74
6	n-C_4H_9	CH_3	$PdCl_2$ (5 mol%), CH_3CN, 80 °C, 0.5 h	**9**	40
6	n-C_4H_9	CH_3	NaOEt (120 mol%), EtOH, 80 °C, 6 h	**9a**	51
6	n-C_4H_9	CH_3	$(PPh_3)_2PdCl_2$ (3.5 mol%), CuI (8 mol%), Et_3N (4 mol equiv.) DMF, N_2, 80 °C, 24 h	—	—
7	n-C_4H_9	Cl	$PdCl_2$ (10 mol%), CH_3CN, 80 °C, 2 h	**10**	71
7	n-C_4H_9	Cl	NaOEt (120 mol%), EtOH, 80 °C, 12 h	**10a**	53

DMF, dimethylformamide.

Still *et al.*[48] reported that *o*-bromo acetanilide exhibited a smooth intermolecular cross-coupling reaction with alkynylstannanes to yield 2-alkyl indoles using organostannaes; however, this also produced toxic metal-containing by-products.[27] Therefore, instead of alkynylstannanes, we use free terminal alkynes, which are environmentally friendly. Another key feature of this procedure is that iodoacetanilides **1** and **2** are employed in the reaction, as Ar–I dominates over Ar–Br or Ar–Cl in reactivity in coupling reaction.[49]

Equilibrium geometries

The optimized structures of compounds **8**, **9**, and **10** are computed at the B3LYP/6-31+G(d, p) level of theory (Fig. 1). The bond distance (Å), bond angle (°), and dihedral angle (°) of compounds **8**, **9**, and **10** are presented in the Supporting Information (Tables S1–S3).

In each indole skeleton, the hetero N forms bonds with three carbon atoms. Among these bonds, N–CO is found to have the lowest values of 1.406 Å in **8** and **9**, which is a direct consequence of the electron-withdrawing tendency of the electronegative oxygen atom. The C1–N28 bond distance (1.424 Å) in **8** and C2–N13 bond distance (1.423 Å) in **9** are consistent with the X-ray structure of indole derivatives reported earlier.[50] However, in indole, this bond distance is shorter, 1.37 Å, indicating that substituent has an impact on the geometry of the indole moiety.[51] On the other hand, the bond distance is slightly longer for entry **10**. Interestingly, the C=O bond distance is 1.222 Å, which is similar for all compounds. Surprisingly, the distance between the two vinyl carbon atoms has the same value of 1.363 Å, and this is also the same for the C–H (1.08 Å) of vinyl group. The distance between the two carbon atoms of benzo-fused rings is 1.411 Å for entries **8** and **9**, whereas it is 1.413 Å for entry **10**. The hydrogen attached to carbon of benzene ring appears to have the C–H distance between 1.079 and 1.087 Å.

The estimated dipole moments of compounds **8**, **9**, and **10** are 3.7288, 3.7077, and 5.6166 Debye, respectively, and the highest negative charges, on the C4 carbon atom of indole nucleus, are −0.726, −0.808, and −0.549 Mulliken, respectively. The electron-withdrawing group in **10** increases the dipole moment and thus makes it more polar.

Thermochemistry

The thermodynamic properties of the isomerization reactions are also computed at the B3LYP/6-31G+(d, p) level of theory, and the results are summarized in Table 2. In the first reaction, the hetero annulations of 2-(1-heptynyl)-4-methyl-*N*-ethanoyl aniline **5** have been carried out in the presence of palladium (II) chloride in acetonitrile to yield 2-pentyl-5-methyl-*N*-ethanoyl indole **8**. The change of electronic energy, enthalpy, and Gibbs free energies of this reaction are −28.67, −28.67, and −25.91 kcal/mol, respectively. Similar values are observed for the second and third reactions. Overall, all cyclization reactions are found to be exothermic.

Frontier molecular orbitals

Energies (eV) of the highest occupied molecular orbital (HOMO) and lowest unoccupied molecular orbital (LUMO) and of the HOMO–LUMO gaps are calculated at the X3LYP/6-31G+(d, p) level of theory for compounds **8–10**. The energy outline of the HOMO, LUMO, and HOMO–LUMO gaps of compounds **8–10** is listed in Table 3. The pictographic presentation of the HOMO and LUMO is illustrated in Fig. 2. The HOMO and LUMO energies of entry **8** are −6.01263 and −1.08216 eV, respectively, with a HOMO–LUMO gap of 4.93047 eV. Entry **9** has almost the same HOMO–LUMO gap of 4.95261 eV as it possesses nearly the same structural feature. The HOMO–LUMO gap of indole is reasonably higher than these compounds, which indicates that these compounds are more chemically reactive than indole.[52] In comparison with entry **8**, the one electron-withdrawing chlorine atom in compound **10** slightly decreases the LUMO energy to −1.24065 eV whereas the HOMO energy is lowered to −6.24321 eV. The HOMO–LUMO gap of entry **10** is 5.00256 eV. The HOMO–LUMO energy gap can be utilized as a simple indicator of kinetic stability. This implies that electron-withdrawing group has a great influence on indole moiety and stabilized the molecular system, thus in turn making compound **10** less reactive. However, electron-releasing groups destabilize the HOMO and LUMO of compounds **8** and **9**, thus promoting greater reactivity.

Vibrational frequencies

For compounds **8**, **9**, and **10**, the experimental and computed vibrational frequencies with their relative intensities are given in Table 4 (IR spectra are included in the Supporting Information (Figs S1–S3)). A characteristic feature of the IR spectra of aromatic compounds is usually observed near 3030 cm^{-1} because of the sp2 C–H stretching vibration. Bands are usually found near

Journal of Physical Organic Chemistry

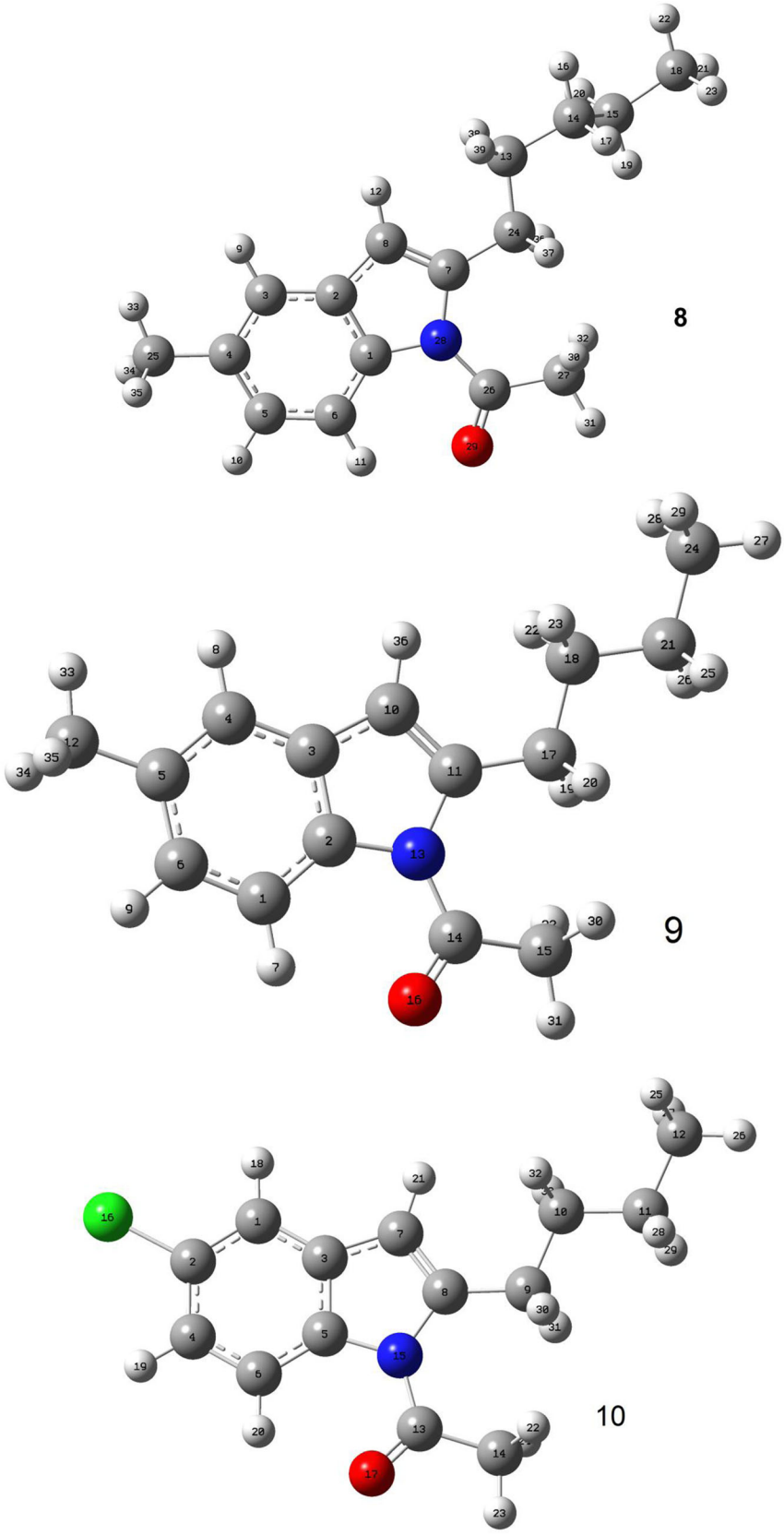

Figure 1. Optimized structures of compounds **8**, **9**, and **10** calculated at the B3LYP/6-31+G(d, p) level of theory

at 1600, 1580, 1500, and 1450 cm^{-1} for in-plane skeletal vibration of aromatic ring.[53] For the entries **8** and **9**, weak bands are observed at 3013 and 3045 cm^{-1}, respectively, which are slightly higher than the computed (scaled) vibrational frequencies 3063 and 3064 cm^{-1}. However, experimental (3108 cm^{-1}) and calculated (3102 cm^{-1}) vibrational frequencies are almost the same for compound **10**. In the case of compounds **8**, **9**, and **10**, a pair of bands at 1591 and 1460, 1591 and 1469, and 1591 and 1487 cm^{-1}, respectively, is observed for the in-plane skeletal vibration of the aromatic ring, which shows a good agreement with computed frequencies of 1603 and 1460, 1603 and 1460, and 1587 and 1547 cm^{-1}. Symmetric and asymmetric C–H stretching vibrational bands are found between 3000 and 2840 cm^{-1} for methyl and methylene groups,[54] and their corresponding computed (scaled) vibrations of compounds **8**, **9**, and **10** are observed at 2926, 2929, and 2929 cm^{-1}, respectively.

The emergence of strong bands in the IR around 1800–1650 cm^{-1} in aromatic compounds is the most salient feature of the existence of the C=O stretching vibration. A comparison of the experimental and computed C=O vibrational frequencies of **8**, **9**, and **10** reveals that the computed (scaled) values (coupled with CH_3) (1688, 1689, and 1693 cm^{-1}, respectively) are almost the same as the experimental values (1688, 1680, and 1686 cm^{-1}, respectively).

Photophysical properties

The electronic absorption spectra of entries **8**, **9**, and **10** are recorded in ethanol, and spectra are shown in the Supporting Information (Figs S4–S6). Experimental and computed absorption properties are presented in Tables 5 and 6.

The absorption properties of indole derivatives are highly sensitive to the indole nucleus.[55] The bands in the UV absorption spectrum of indole in 95% ethanol occur at 287, 266, and 216 nm, and a recent study of *N*-acyl indole demonstrated absorption at 297, 288, and 238 nm.[56] The experimental absorptions (strong) of compound **8** are found at 304, 300, and 294 nm. The computed absorptions calculated at the X3LYP/6-31+G(d, p) level of theory are found at 290, 271, 246, and 232 nm, which shows good agreement with the experimental results. The most intense peak is contributed from excitation of electrons from HOMO to LUMO (75.01%). For compound **9**, peaks of weaker intensity are found at 304 and 296 nm. The corresponding calculated peaks are observed at 288, 270, 245, and 232 nm.

Table 2. Thermodynamic properties (change of energy, enthalpy, and Gibbs free energy in kcal/mol) of all cyclization reactions

Entry	1	2	3
ΔE	−28.67	−28.70	−28.80
ΔH	−28.67	−28.70	−28.80
ΔG	−25.91	−25.07	−25.94

Table 3. The energy (eV) of HOMO, LUMO, and HOMO–LUMO gaps of compounds **8–10**

Molecular orbital	8	9	10	Indole
LUMO +2	0.36126	0.10692	0.04563	0.392388
LUMO +1	−0.39474	−0.37341	−0.71982	−0.12871
LUMO	−1.08216	−1.05813	−1.24065	−0.47266
HOMO	−6.01263	−6.01074	−6.24321	−5.76446
HOMO −1	−6.35877	−6.36012	−6.56019	−6.21944
HOMO −2	−7.62642	−7.6383	−7.75764	−7.73375
Gap	4.93047	4.95261	5.00256	5.29179

HOMO, highest occupied molecular orbital; LUMO, lowest unoccupied molecular orbital.

Absorption at 245 nm arises from excitation of electrons from HOMO to LUMO +1 (74.01%) transition. The replacement of methyl group by chlorine at 5-position exerts a negative inductive effect and increases the intensity. The maximum wavelength observes at 237 nm contributed from HOMO −1 to LUMO +1 (83.21%) transition. It is evident from Table 5 that a small increment of the alkyl chain (–CH_2–) also causes red shift along with a substantial hyperchromic effect for compound **8**. However, removal of one alkyl chains at 2-position exhibits a large bathochromic shift for compound **9**.

NMR

The experimental and calculated NMR at B3LYP/6-311+G(2d, p) is presented in the Supporting Information (Figs S7–S13 and Tables S4–S6, NMR atom numbering is indicated in the Fig S7). The computed values of the singlet signals found at 8.91, 8.90, and 8.99 ppm for compounds **8**, **9**, and **10** are assigned to H27, H9, and H17, respectively. However, experimental values 7.685, 7.6825, and 7.8045 ppm are slightly lower than the computed results. Similar trends for experimental and computed chemical shifts are observed for the remaining proton present in the benzene ring. The experimental δ values (6.327, 6.325, and 6.343 ppm) of vinyl proton (H35, H13, and H21) present in the pyrrole ring of entries **8**, **9**, and **10,** whereas the calculated values of those protons are found to resonate at 6.5891, 6.6004, and 6.6911 ppm, respectively. The methylene protons in the vicinity of indole nucleolus of compounds **8**, **9**, and **10** are resonated between 2.99 and 2.97 ppm, which shows a good correlation to the calculated chemical shift. Overall, the recorded ^{1}H NMR chemical shifts of compounds **8**, **9**, and **10** demonstrate a very good correspondence with the calculated chemical shifts.

Nevertheless, the carbonyl carbon C=O has a low-lying excited state involving the movement of electrons from the oxygen lone pair to the anti-bonding p orbital that generates a paramagnetic current. This $n \rightarrow \pi^*$ transition causes the large shift to high frequency, and thus, the carbonyl carbon has a smaller intensity and appears in a characteristic field, 150–220 ppm,[57,58] making it easier to recognize the carbonyl absorption from the other resonances. In this study, low-field shift of carbonyl carbons C29, C27, and C11 was recorded in ^{13}C NMR spectrum at 170.19, 170.195, and 170.052 for compounds **8**, **9**, and **10**, respectively. The ring carbon atom of compounds **8**, **9**, and **10** attached to hydrogen atoms is resonated from 124.599 to 104.037 ppm, similar to the computed values. In the experimental ^{13}C spectrum of compounds **8**, **9**, and **10**, the peak intensities of the methyl carbon are similar to or slightly smaller than those of the methylene carbon. The experimental values of carbon of three methyl groups C30, C22, and C4 are found at 27.573, 21.122, and 14.045 ppm, and their corresponding computed values are observed at 29.225, 22.0473, and 15.8026 ppm. On the other hand, the experimental values of methylene carbon are 31.678, 30.553, 28.626, and 22.56 ppm whereas the calculated values are 35.682, 33.665,

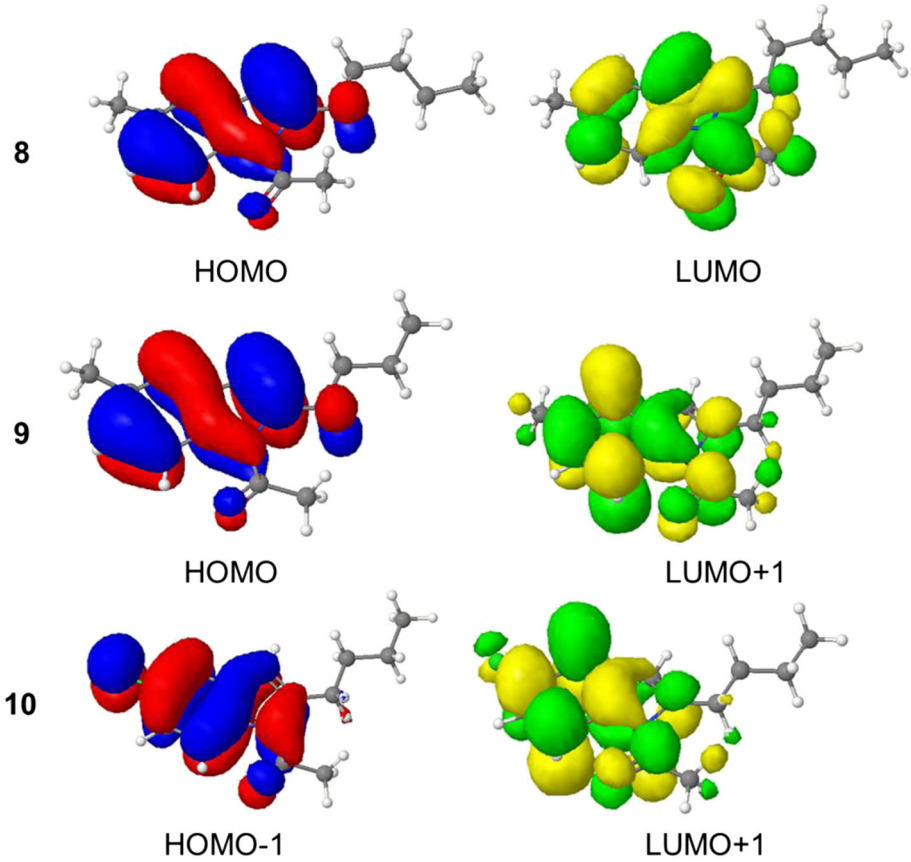

Figure 2. Selected HOMO and LUMO of compounds **8**, **9**, and **10**

Table 4. Selected experimental and calculated (without and with scaling) vibrational frequencies (cm^{-1}) of compounds **8–10**

Experimental	Frequencies without scaling (intensity)	Frequencies with scaling[a]	Assignments[b]
	Compound **8**		
3014	3175 (21)	3063	ν sp^2C–H
2922	3033 (49)	2926	ν_{sym} sp^3C–H
1688	1750 (256)	1688	ν C=O + ωCH_3
1591	1661 (14)	1603	ν C=C + β sp^2C–H
1460	1514 (22)	1460	ν C=C + β sp^2C–H + s CH_2
1373	1420 (2)	1370	ω CH_3
1315	1338 (336)	1291	ν C–N + ω CH_3 + β sp^2C–H
816	830 (46)	801	γ sp^2C–H
737	745 (2)	719	r CH_2
	Compound **9**		
3046	3176 (21)	3064	ν sp^2C–H
2959	3073 (8)	2965	ν_{sym} CH_3
2936	3035 (71)	2929	ν_{sym} CH_3 + ν_{sym} CH_2
1680	1751 (259)	1689	ν C=O + ω CH_3
1591	1661 (14)	1603	ν C=C + β sp^2C–H
1469	1513 (41)	1460	ν C=C + β sp^2C–H + ω CH_3
1369	1424 (7)	1373	ω CH_3
1317	1339 (248)	1292	ν C–N + β sp^2C–H + ω CH_3
824	834 (26)	805	γ sp^2C–H + r CH_2
	Compound **10**		
3108	3215 (5)	3102	ν sp^2C–H
2937	3036 (76)	2929	ν_{sym} CH_3
1686	1755 (250)	1693	ν C=O + ω CH_3
1591	1645 (44)	1587	ν C=C + β sp^2C–H
1487	1603 (3)	1547	ν C=C + β sp^2C–H
1371	1422 (7)	1372	ω CH_3
1317	1335 (354)	1306	ν C–N + β sp^2C–H+ ω CH_3
829	829 (36)	799	γ sp^2C–H + r CH_2

[a]Scaling factor for B3LYP/6-31G+(d, p) is 0.9648.
[b]ν, stretching; ν_{sym}, symmetric stretching; β, in-plane bending; γ, out-plane bending; r, rocking; ω, bending.

Table 5. Experimental absorption properties of compounds **8**, **9**, and **10**

Compound	Substituent on indoles nucleus			λ nm(Abs)
	1	**2**	**5**	
8	–CO–CH_3	–$(CH2)_4CH_3$	–CH_3	304.0(0.352), 300.3(0.323), 293.5(0.364)
9	–CO–CH_3	–$(CH2)_3CH_3$	–CH_3	366.5(0.005), 304.0(0.204), 295.5(0.208)
10	–CO–CH_3	–$(CH2)_3CH_3$	–Cl	352.5(0.005), 305.0(0.350), 291.0(0.436)

31.027, and 26.276 ppm, which implies that the calculated values are slightly higher than the experimental ones. However, compounds **9** and **10** exhibit a similar correlation with the calculated and experimental results for both methyl and methylene carbons.

Based on the ^{1}H and ^{13}C chemical shift data presented in the Supporting Information (Tables S4–S6), it can be deduced that the qualitative proton and carbon NMR chemical shifts of the studied indole derivatives are described fairly well by the selected method along with the basis set. The correlation between the experimental and calculated chemical shifts is obtained by B3LYP/6-311+G(2d, p), which is depicted in Fig. 3.

Mechanistic study

The distinctive palladium-catalyzed reactions start with the formation of a π-complex between Pd(II) salt and the alkenes or alkynes. The Pd–π complex significantly diminished the electron density at the C=C or C≡C bonds, which eventually promotes cyclization and proton transfer by facilitating the intermolecular or intramolecular nucleophilic attack.[27,59,60] In this mechanistic study, we focus on the cyclization and subsequent proton transfer. Palladium (II) chloride-based cyclization proceeds via a two-step reaction. In the first transition state, one proton is transferred from the –NH group to the alkyne carbon. The breaking N–H bond distance is 1.37 Å, and the forming =C–H bond distance is 1.25 Å (Fig. 4). Moreover, the amino nitrogen simultaneously approaches to the ethylene carbon for cyclization with a C–N bond distance of 2.26 Å. The palladium is attached to the other ethylene carbon and promotes the overall proton transfer and cyclization. In this concerted mechanism, both proton

Table 6. Calculated absorption properties of compounds **8**, **9**, and **10** at X3LYP/6-31+G(d, p) level of theory including ethanol as a solvent

Wavelength (nm)	Excitation energies (eV)	Oscillator strengths	Molecular orbital contribution
			Compound **8**
289.97	4.2757	0.1454	H-1 → L + 1 (3.02%), H → L (91.15%), H → L + 1 (5.1%)
271.48	4.5669	0.0814	H-1 → L (81.41%), H → L + 1 (11.97%), H → L + 7 (2.08%)
248.7	4.9852	0.0044	H-3 → L (2.72%), H-2 → L (83.16), H-2 → L + 1 (7.21%), H-2 → L + 7 (2.21%)
246.17	5.0364	0.3185	H-1 → L (12.14%), H-1 → L + 7 (2.99%), H → L (3.31%), H → L (75.16%)
233.4	5.3121	0.0737	H-1 → L + 1 (18.72%), H → L + 2 (69.85%), H → L + 3 (2.71%)
232.8	5.3257	0.1806	H-1 → L + 1 (63.2%), H → L + 2 (21.01%), H → L + 7 (4.73%)
217.51	5.7003	0.0033	H-1 → L + 2 (75.5%), H-1 → L + 3 (6.35%), H-1 → L + 4 (5.06%), H → L + 3 (8.58%)
217.34	5.7046	0.0001	H-1 → L + 2 (7.82%), H → L + 2 (2.65%), H → L + 3 (84.02%)
214.55	5.7789	0.0021	H → L + 4 (80.08%), H → L + 5 (6.27%), H → L + 6 (6.06%)
210.19	5.8986	0.0198	H-3 → L (40.79%), H → L + 6 (6.99%), H → L + 7 (44.45%)
			Compound **9**
288.19	4.3021	0.146	H-1 → L + 1 (3.09%), H → L (90.74%), H → L + 1 (5.36%)
270.16	4.5893	0.0809	H-1 → L (80.19%), H → L + 1 (12.88%), H → L + 8 (2.66%)
246.75	5.0247	0.0048	H-2 → L (84.24%), H-2 → L + 1 (7.41%), H-2 → L + 5 (3.58%)
245.18	5.0568	0.3115	H-1 → L (13.08%), H-1 → L + 5 (3.43%), H → L (3.19%), H → L + 1 (74.01%)
231.97	5.3449	0.0103	H → L + 2 (90.68%), H → L + 3 (3.22%), H → L + 6 (2.44%)
231.58	5.3538	0.2585	H-1 → L (2.17%), H → L (81.04%), H-1 → L (2.36%), H → L + 5 (7.15%)
217.12	5.7105	0.0012	H → L + 2 (3.06%), H → L + 3 (93.21%)
216.69	5.7218	0.0022	H-1 → L + 2 (85.33%), H-1 → L + 3 (8.71%)
212.14	5.8444	0.002	H → L + 4 (74.85%), H → L + 6 (13.68%), H → L + 8 (6.76%)
209.35	5.9223	0.0328	H-3 → L (44.88%), H → L + 5 (34.64%), H → L + 7 (13.58%)
			Compound **10**
285.17	4.3477	0.1413	H-1 → L + 1 (4.48%), H → L (84.86%), H → L + 1 (8.67%)
270.54	4.5828	0.0585	H-1 → L (70.33%), H → L (6.09%), H → L + 1 (18.78%), H → L + 5 (2.33%)
250.66	4.9464	0.2043	H-2 → L (13.11%), H-2 → L + 1 (2.37%), H-1 → L (16.05%), H-1 → L + 5 (2.14%), H → L (3.03%), H → L + 1 (56.76%)
249.49	4.9695	0.0449	H-2 → L (70.03%), H-2 → L + 1 (6.68%), H-2 → L + 5 (3.48%), H-1 → L (4.88%), H → L + 1 (10.27%)
237.13	5.2285	0.4024	H-1 → L (3.05%), H-1 → L + 1 (83.21%), H → L (3.92%), H → L + 5 (4.37%)
224.62	5.5197	0.0052	H → L + 2 (93.45%)
215.04	5.7655	0.0003	H-1 → L + 4 (2.55%), H → L + 4 (90.27%)
212.97	5.8216	0.0022	H-1 → L + 2 (45.09%), H-1 → L + 4 (46.85%), H → L + 4 (2.53%)
210.5	5.89	0.0028	H-1 → L + 2 (32.93%), H-1 → L + 3 (10.18%), H-1 → L + 4 (27.53%), H → L + 3 (24.72%)
209.94	5.9056	0.0028	H-1 → L + 2 (32.93%), H-1 → L + 3 (10.18%), H-1 → L + 4 (27.53%), H → L + 3 (24.72%)

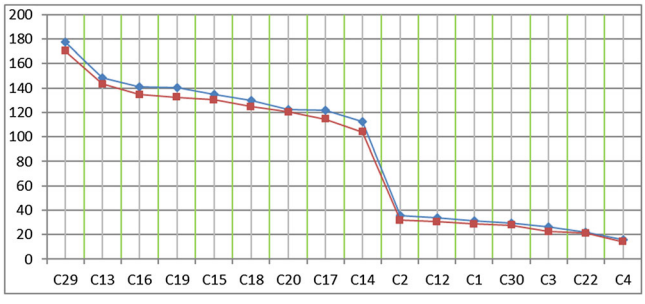

Figure 3. Correlation between experimental (red) and calculated (blue) chemical shift ^{13}C NMR of compound **8**

transfer and cyclization occur synchronously, which is also a common feature in various concerted reactions.[61] In the second transition state, one proton is transferred from one of the ethylene carbon atoms to the other. The breaking C–H bond distance is 1.40 Å, and forming C–H bond distance is 1.35 Å. The gas-phase activation barrier of the first transition state is 37 kcal/mol, which appears to be the rate-determining step (Fig. 5). The barrier height of the second transition state is 28 kcal/mol, which indicates that proton transfer between the two carbon atoms occurs faster as compared with the proton transfer between nitrogen and carbon. Incorporation of a solvent (acetonitrile) by the SMD solvation model further reduces the barrier height of the rate-determining step to 31 kcal/mol. However, the CPCM solvation model fails to lower the barrier height. Overall, the palladium-based cyclization reaction of anilines to indoles is exothermic.

The effect of substitution on the transition states of this reaction is also considered by replacing the $-CH_3$ group (**9**) with an electron-withdrawing –Cl group (**10**). The gas-phase barrier height of the first transition state is slightly higher (−38 kcal/mol) than the $-CH_3$ substituent pathway. Solvent (acetonitrile) has little influence on the barrier height (37 kcal/mol) of the rate-determining step contrary to the $-CH_3$ substituent pathway

Journal of Physical Organic Chemistry

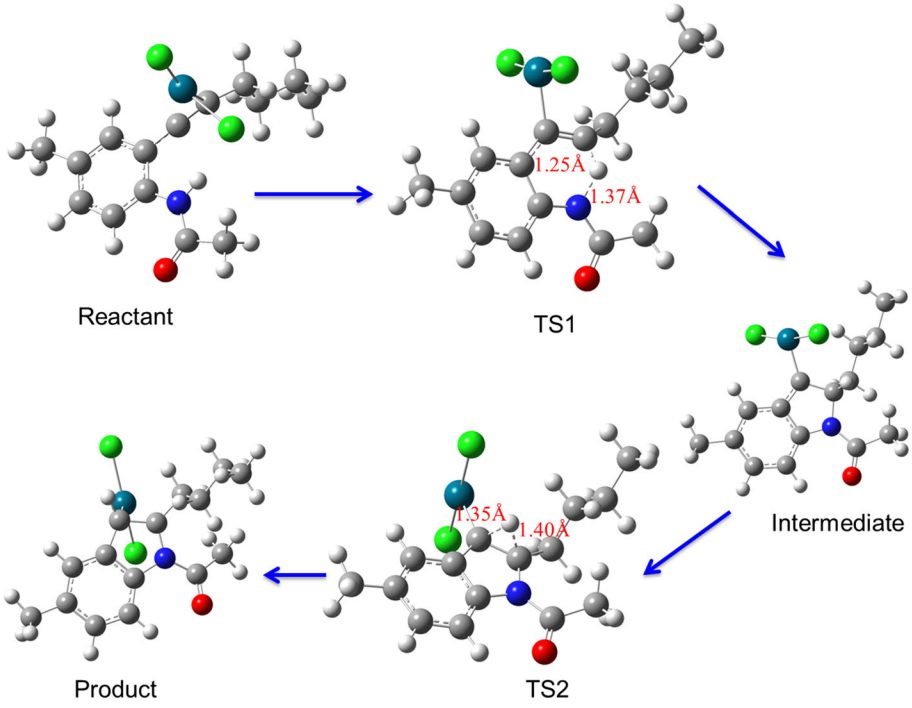

Figure 4. Two-step concerted mechanism of palladium-catalyzed cyclization of 2-alkynyl-4-substituted-*N*-ethanoyl anilines to indoles, computed at B3LYP/SDD level of theory

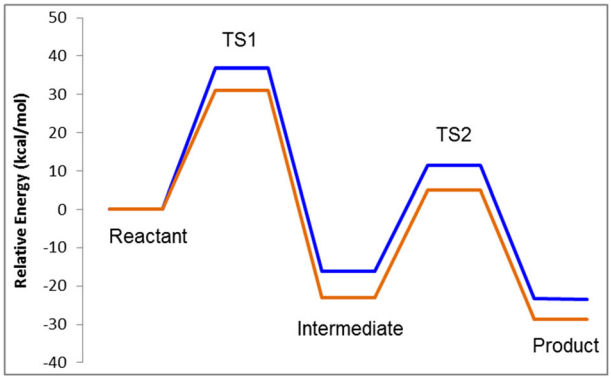

Figure 5. Relative energy (kcal/mol) diagram of palladium-catalyzed cyclization computed at B3LYP/SDD level of theory. Blue and orange lines represent the gas and solvent phase barrier heights, respectively

(Fig. S14). The gas-phase and solvent-mediated barrier heights of the second transition state are 26 and 27 kcal/mol, respectively. These results suggest that the electron-releasing $-CH_3$ group promotes the Pd-catalyzed C–N cyclization to indoles compared with the electron-withdrawing –Cl group in the presence of acetonitrile, which is in complete agreement with our experimental finding. Although the main driving force of Pd-catalyzed reactions depends on several factors including solvent, temperature, and substitutes, these results show that solvent has great influence on C–N coupling and proton transfer.

CONCLUSION

Palladium-catalyzed cross-coupling and isomerization reactions are developed to produce indole derivatives **8–10**. For cross-coupling reaction, free terminal alkynes and substituted 2-iodoacetanilides, which form distinct halogen bonding, have been used for synthesis of substituted anilines **5–7**. Overall, the strategy allows the facile preparation of 5-substituted-2-alkyl-*N*-ethanoyl indoles, which may be applied to prepare other *N*-alkanoyl indoles. The calculated energy and enthalpy of these reactions related to products **8–10** are nearly the same as −28.67 kcal/mol. The optimized geometries of **8–10** demonstrate that the substituents attached to an indole framework have an influence on their structure. Introduction of a Cl group at the 5-position in **10** slightly increases the HOMO–LUMO gap as compared with the gaps of **8** and **9**. The lower HOMO–LUMO gaps in **8** and **9** suggest that they are more chemically reactive than **10**. Reduction of one $-CH_2-$ group in **9** decreases the absorption compared with **8**; however, the replacement of methyl group by chlorine at the 5-position increases the absorption. Experimental IR and NMR studies are in good agreement with the DFT calculations. Cyclization of 2-alkynyl-4-substituted-*N*-ethanoyl anilines to indole **9** by the palladium catalyst follows a two-step concerted mechanism in which the gas-phase activation energies of TS1 and TS2 are 37 and 28 kcal/mol, respectively. Solvent (acetonitrile) further decreases the activation energy of the rate-determining step to 31 kcal/mol. The relative energy profile reveals that cyclization and proton transfer occur synchronously in step one, which is assumed to be the rate-limiting step. Moreover, an electron-withdrawing group has a smaller influence on the barrier height of this reaction compared with the electron-releasing group.

Acknowledgements

We acknowledge the financial assistance of Ministry of National Science Information and Communication Technology, Bangladesh. We are thankful to Bangladesh Council of Scientific and Industrial Research (BCSIR), Dhaka, for taking NMR spectra. We are also grateful to our donors who are helping to build a computational platform in Bangladesh http://computchembiochem.com/1_8_Donate.html. We are also thankful to Professor Raymond Poirier, Department of Chemistry, Memorial University, Canada, and the Atlantic Computational Excellence Network for allocating computational resource to NMR calculation. Authors like to thank Dr Steven Daly, Institut Lumière Matière, CNRS et Université Lyon 1, Villeurbanne 69100, France, for reading this manuscript.

REFERENCES

[1] M. Somei, F. Yamada, *Nat. Prod. Rep.* **2005**, *22*, 73–103.
[2] B. E. Evans, K. E. Rittle, M. G. Bock, R. M. DiPardo, R. M. Freidinger, W. L. Whitter, G. F. Lundell, D. F. Veber, P. S. Anderson, *J. Med. Chem.* **1988**, *31*, 2235–2246.
[3] D. A. Horton, G. T. Bourne, M. L. Smythe, *Chem. Rev.* **2003**, *103*, 893–930.

[4] J. J. Li, G. W. Gribble, *Palladium in Heterocyclic Chemistry*, 2nd edn, Elsevier Press, Amsterdam, **2007**.
[5] J. T. Kuethe, A. Wong, C. Qu, J. Smitrovich, I. W. Davies, D. L. Hughes, *J. Org. Chem.* **2005**, *70*, 2555–2567.
[6] M. C. Van Zandt, M. L. Jones, D. E. Gunn, L. S. Geraci, J. H. Jones, D. R. Sawicki, J. Sredy, J. L. Jacot, A. T. DiCioccio, T. Petrova, A. Mitschler, A. D. Podjarny, *J. Med. Chem.* **2005**, *48*, 3141–3152.
[7] T. Kawasaki, K. Higuchi, *Nat. Prod. Rep.* **2005**, *22*, 761–793.
[8] G. R. Humphrey, J. T. Kuethe, *Chem. Rev.* **2006**, *106*, 2875–2911.
[9] A. Frazer, J. G. Hensler, *In Siegel, Basic Neurochemistry*, 6th edn, Lippincott Williams and Wilkins, Philadelphia, USA, **1999**.
[10] R. L. Noble, C. T. Beer, J. H. Cutts, *Ann. N. Y. Acad. Sci.* **1958**, *76*, 882.
[11] G. H. Svoboda, N. Neuss, M. Gorman, *J. Am. Pharm. Assoc. Sci. Ed.* **1959**, *48*, 659.
[12] T. Kuboyama, H. Tokuyama, T. Fukuyama, *Pure Appl. Chem.* **2003**, *75*, 29–38.
[13] P. Neuvonen, J. Backman, M. Niemi, *Clin. Pharmacokinet.* **2008**, *47*, 463–474.
[14] G. La Regina, A. Coluccia, F. Piscitelli, A. Bergamini, A. Sinistro, A. Cavazza, G. Maga, A. Samuele, S. Zanoli, E. Novellino, M. Artico, R. Silvestri, *J. Med. Chem.* **2007**, *50*, 5034–5038.
[15] F.-R. Alexandre, A. Amador, S. Bot, C. Caillet, T. Convard, J. Jakubik, C. Musiu, B. Poddesu, L. Vargiu, M. Liuzzi, A. Roland, M. Seifer, D. Standring, R. Storer, C. B. Dousson, *J. Med. Chem.* **2010**, *54*, 392–395.
[16] S. Prabhu, Z. Akbar, F. Harris, K. Karakoula, R. Lea, F. Rowther, T. Warr, T. Snape, *Bioorg. Med. Chem.* **2013**, *21*, 1918–1924.
[17] P. Grewal, M. Mallaney, K. Lau, A. Sreedhara, *Mol. Pharm.* **2014**, *11*, 1259–1272.
[18] M. K. Nazeeruddin, *Coord. Chem. Rev.* **2004**, *248*, 1161–1164.
[19] N.-G. Park, M. G. Kang, K. M. Kim, K. S. Ryu, S. H. Chang, D.-K. Kim, J. van de Lagemaat, K. D. Benkstein, A. J. Frank, *Langmuir* **2004**, *20*, 4246–4253.
[20] P. V. Kamat, M. Haria, S. Hotchandani, *J. Phys. Chem. B* **2004**, *108*, 5166–5170.
[21] A. Furube, R. Katoh, T. Yoshihara, K. Hara, S. Murata, H. Arakawa, M. Tachiya, *J. Phys. Chem. B* **2004**, *108*, 12583–12592.
[22] Y. Saito, N. Fukuri, R. Senadeera, T. Kitamura, Y. Wada, S. Yanagida, *Electrochem. Commun.* **2004**, *6*, 71–74.
[23] Q. Li, L. Lu, C. Zhong, J. Shi, Q. Huang, X. Jin, T. Peng, J. Qin, Z. Li, *J. Phys. Chem. B* **2009**, *113*, 14588–14595.
[24] R. J. Sundberg, *The Chemistry of Indoles*, Academic Press, New York, **1970**.
[25] R. J. Sundberg, *Indoles*, Academic Press, London, **1996**.
[26] G. W. Gribble, *J. Chem. Soc. Perkin Trans. 1* **2000**, 1045–1075.
[27] S. Cacchi, G. Fabrizi, *Chem. Rev.* **2005**, *105*, 2873–2920.
[28] L. S. Hegedus, *Angew. Chemie Int. Ed. English* **1988**, *27*, 1113–1126.
[29] G. Zeni, R. C. Larock, *Chem. Rev.* **2004**, *104*, 2285–2310.
[30] I. Nakamura, Y. Yamamoto, *Chem. Rev.* **2004**, *104*, 2127–2198.
[31] M. C. Willis, G. N. Brace, I. P. Holmes, *Angew. Chemie Int. Ed.* **2005**, *44*, 403–406.
[32] J. Barluenga, M. A. Fernández, F. Aznar, C. Valdés, *Chem. An Eur. J.* **2005**, *11*, 2276–2283.
[33] Y.-Q. Fang, M. Lautens, *Org. Lett.* **2005**, *7*, 3549–3552.
[34] C. Mukai, Y. Takahashi, *Org. Lett.* **2005**, *7*, 5793–5796.
[35] N. Kambe, T. Iwasaki, J. Terao, *Chem. Soc. Rev.* **2011**, *40*, 4937–4947.
[36] Y. Wei, I. Deb, N. Yoshikai, *J. Am. Chem. Soc.* **2012**, *134*, 9098–9101.
[37] M. W. Khan, A. F. G. M. Reza, *Tetrahedron* **2005**, *61*, 11204–11210.
[38] M. Wahab Khan, M. Jahangir Alam, M. A. Rashid, R. Chowdhury, *Bioorg. Med. Chem.* **2005**, *13*, 4796–4805.
[39] M. W. Khan, A. Akther, M. S. Alam, *Synlett* **2014**, *25*, 831–834.
[40] F. R. Heck, *Palladium Reagents in Organic Synthesis: Best Synthetic Methods*, Academic Press, New York, USA, **1985**.
[41] M. J. Frisch, G. W. Trucks, H. B. Schlegel, G. E. Scuseria, M. A. Robb, J. R. Cheeseman, G. Scalmani, V. Barone, B. Mennucci, G. A. Petersson, H. Nakatsuji, M. Caricato, X. Li, H. P. Hratchian, A. F. Izmaylov, J. Bloino, G. Zheng, J. L. Sonnenberg, M. Hada, M. Ehara, K. Toyota, R. Fukuda, J. Hasegawa, M. Ishida, T. Nakajima, Y. Honda, O. Kitao, H. Nakai, T. Vreven, J. A. Montgomery Jr., J. E. Peralta, F. Ogliaro, M. Bearpark, J. J. Heyd, E. Brothers, K. N. Kudin, V. N. Staroverov, R. Kobayashi, J. Normand, K. Raghavachari, A. Rendell, J. C. Burant, S. S. Iyengar, J. Tomasi, M. Cossi, N. Rega, J. M. Millam, M. Klene, J. E. Knox, J. B. Cross, V. Bakken, C. Adamo, J. Jaramillo, R. Gomperts, R. E. Stratmann, O. Yazyev, A. J. Austin, R. Cammi, C. Pomelli, J. W. Ochterski, R. L. Martin, K. Morokuma, V. G. Zakrzewski, G. A. Voth, P. Salvador, J. J. Dannenberg, S. Dapprich, A. D. Daniels, Ö. Farkas, J. B. Foresman, J. V Ortiz, J. Cioslowski, D. J. Fox, *Gaussian* 09, Revision *A.02*, Gaussian, Inc., Wallingford, **2009**.
[42] J. P. Merrick, D. Moran, L. Radom, *J. Phys. Chem. A* **2007**, *111*, 11683–11700.
[43] M. A. Halim, D. M. Shaw, R. A. Poirier, *J. Mol. Struct. (THEOCHEM)* **2010**, *960*, 63–72.
[44] M. Barone, M. Cossi, *J. Phys. Chem. A* **1998**, *102*, 1995–2001.
[45] M. Cossi, N. Rega, G. Scalmani, V. Barone, *J. Comp. Chem.* **2003**, *24*, 669–681.
[46] A. V. Marenich, C. J. Cramer, D. G. Truhlar, *J. Phys. Chem. B* **2009**, *113* 6378–6396.
[47] M. M. Hoque, M. A. Halim, M. M. Rahman, M. I. Hossain, M. W. Khan, *J. Mol. Struct.* **2013**, *1054-1055*, 367–374.
[48] D. E. Rudisill, J. K. Stille, *J. Org. Chem.* **1989**, *54*, 5856–5866.
[49] R. Chinchilla, C. Nájera, *Chem. Rev.* **2007**, *107*, 874–922.
[50] O. F. Vázquez-Vuelvas, J. V. Hernández-Madrigal, R. Gaviño, M. A. Tlenkopatchev, D. Morales-Morales, J. M. Germán-Acacio, Z. Gomez-Sandoval, C. Garcias-Morales, A. Ariza-Castolo, A. Pineda-Contreras, *J. Mol. Struct.* **2011**, *987*, 106–118.
[51] L. Pejov, V. Stefov, B. Šoptrajanov, *Vib. Spectrosc.* **1999**, *18*, 435–439.
[52] J. Aihara, *J. Phys. Chem. A* **1999**, *103*, 7487–7495
[53] B. S. Furniss, A. J. Hannafort, P. W. Smith, A. R. Tatchell, *Vogel's Textbook of Practical Organic Chemistry*, 5th edn, Longman Group Ltd., UK, **2006**.
[54] D. L. Pavia, G. L. Lampman, G. S. Kris, *Introduction to Spectroscopy*: *A Guide for Students of Organic Chemistry*, 3rd edn, Harcourt College Publishers, Fort Worth, **2001**.
[55] W. J. Houlihan, *The Chemistry of Heterocyclic Compounds*, 25th edn, John Wiley & Sons, Inc., New York, **1979**.
[56] M. N. Ibrahim, *E-J. Chem.* **2007**, *4*, 415–418.
[57] M. Venkatanarayana, P. K. Dubey, *Synth. Commun.* **2011**, *42*, 1746–1759.
[58] J. S. Yadav, B. V. S. Reddy, A. K. Basak, B. Visali, A. V. Narsaiah, K. Nagaiah, *Eur. J. Org. Chem.* **2004**, 546–551.
[59] M. Platon, R. Amardeil, L. Djakovitch, J. C. Hierso, *Chem. Soc. Rev.* **2012**, *41*, 3929–3968.
[60] T. Ghebreghiorgis, B. H. Kirk, A. Aponick, D. H. Ess, *J. Org. Chem.* **2013**, *78*, 7664–7673.
[61] M. A. Halim, M. H. Almatarneh, R. A. Poirier, *J. Phys. Chem. B* **2014**, *118*, 2316–2330.

SUPPORTING INFORMATION

Additional supporting information may be found in the online version of this article at the publisher's web-site.